Iranian Journal of Materials Forming 10 (2) (2023) 4-11

IJMOF

Online ISSN: 2383-0042

Iranian Journal of Materials Forming

Journal Homepage: http://ijmf.shirazu.ac.ir

Research Article

# Integral Hydro-Bulge Forming of Spherical Vessels: A Numerical and Experimental Study

H. Deilami Azodi[1*], J. Rezaei[1], A. Zeinolabedin-Beygi[2] and H. Badparva[3]

[1] Department of Mechanical Engineering, Arak University of Technology, Arak, Iran
[2] Department of Mechanical Engineering, Tarbiat Modares University, Tehran, Iran
[3] Department of Mechanical Engineering, Khajeh Nasir al-Din Tusi University of Technology, Tehran, Iran

ARTICLE INFO

*Article history:*

Received 28 February 2023
Reviewed 3 April 2023
Revised 17 April 2023
Accepted 17 May 2023

*Keywords:*

Integral hydro-bulge forming
Shell hydroforming
Lateral petals
Thickness distribution
Critical fluid pressure

*Please cite this article as:*

H. Deilami Azodi, J. Rezaei, A. Zeinolabedin-Beygi, H. Badparva, Integral hydro-bulge forming of spherical vessels: a numerical and experimental study, *Iranian Journal of Materials Forming*, 10(2) (2023) 4-11.

ABSTRACT

The integral hydro-bulge forming (IHBF) process, also called shell hydroforming, is a die-less forming technique used to manufacture hollow parts from preforms made of sheet blanks cut and welded together. In this study, integral hydro-bulging of spherical vessels was investigated both numerically and experimentally. Numerical simulations were performed using Abaqus commercial software, and the numerical results were validated via comparison with those obtained from the experiments. The thickness distribution along the equatorial and meridian paths, sphericity of the formed vessel, and critical fluid pressure at which instability occurs were studied, and the effect of the number of lateral petals was investigated. For this study, an St12 steel sheet with a thickness of 0.8 mm was used to make a spherical shell with 12 lateral petals and a diameter of 400 mm. The results showed that the use of preforms with more lateral petals leads to a more uniform thickness distribution and shape accuracy in the formation of spherical vessels. Furthermore, by increasing the number of petals from 8 to 16, the thickness decreased by 4.2%. The maximum thickness reduction occurs in the 8-petal state, and the least thickness reduction occurs in the 12-petal state. The results show that the increase in the number of lateral petals leads to the increase in the critical fluid pressure. By doubling the number of lateral petals, fracture pressure increased by 74% consequently.



## 1. Introduction

Metal forming processes such as single-point incremental forming [1], bending [2], rubber pad forming [3], roll forming [4], hydromechanical deep drawing [5], and laser forming [6] can be used to produce metal parts. In hydroforming processes, as a type of soft tool forming technology, fluid pressure is utilized instead of conventional mechanical forces to form complicated shapes. Hydroforming has many advantages over common forming processes, including improved mechanical properties, less thinning, better surface finish, fewer components required in an assembly, and less rework owing to the formation of geometries closer to the final shape [7]. These advantages have led to their increased use in various

* Corresponding author
E-mail address: hdazodi@arakut.ac.ir (H. Deilami Azodi)
https://doi.org/10.22099/IJMF.2023.46935.1250

industries. The hydroforming process is divided into three categories: tube hydroforming, sheet hydroforming, and shell hydroforming or integral hydro-bulge forming (IHBF). The IHBF is a free hydro-bulging process without any dies. It can be very useful to form large hollow parts while eliminating die costs. This process is used to manufacture hollow geometries, such as spherical, elliptical, and ring-shaped vessels, from a preform made of welded petals. Compared with other categories of hydroforming, fewer studies have been conducted on shell hydroforming.

Zhang et al. [8] studied the manufacturing of closed spherical vessels by shell hydroforming process and investigated the stress and strain distribution in formed sheets. Zhang et al. [9] investigated the hydro-bulging of a spherical vessel made of 32-sided polygonal shell consisting of 20 hexagonal, and 12 pentagonal flat sheets. The stress and strain distributions in the shells were experimentally measured. They found that the relationship between the deformation of the center of the blanks and pressure was almost linear. That is, the larger the blanks, the larger is the deformation. Teng et al. [10] investigated the role of the initial structure in preventing wrinkling within the hydro-forming process of large elbows. Their results showed that choosing an appropriate initial structure can prevent wrinkles. Hu and Wang [11] studied the effect of shape, number and preform type of shell segments in hydro-bulging of spheroidal vessels. Wang et al. [12] studied the shell hydroforming process and its application. The authors also introduced the principle of preforming shell segments before hydro-bulging of the vessel. They mentioned that in the hydro-bulging process, plastic deformation begins from the center of a flat petal where the curvature radius is infinite. Subsequently, the curvature increased correspondingly. Thereafter, plastic deformation occurred at positions with a relatively larger radius of curvature. By repeating this sequence of deformations, the entire shell is deformed into a sphere with a uniform radius. Yuan et al. [13] studied the hydroforming of elliptical shells with a large axis length ratio and proposed a two-step IHBF technique for manufacturing shells with the length ratio of the long axis to the short axis larger than 1.4. Using the proposed technique, they obtained an ellipsoidal shell with an axis length ratio of 1.8. Yuan et al. [14] studied the wrinkling in the hydro-bulging process of the elliptical shells. They designed a combined ellipsoidal shell as the preform shell to prevent wrinkling during the hydroforming of ellipsoidal shells with an axis-length ratio greater than $\sqrt{2}$. Zhang and Wang [15] studied the die-less shell hydro-bulging both experimentally and numerically. The roundness of the formed spherical shell was improved using the “corner-cutting treatment” of the panels. For the first time, they considered the thickness of the weld line in a numerical simulation of shell hydro-bulging. Zhang and Yuan [16] investigated the axis length changes during hydroforming of the combined ellipsoidal shell to obtain a reasonable preform. For a parametric study of the preform shells, they performed numerical simulations with different structural parameters according to the Box-Behnken method. A mathematical response model was developed based on regression analysis between the axis lengths and structural parameters. Zhang et al. [17] studied the effect of preform type in hydroforming of spherical shells. A numerical simulation was used to analyze the roundness of the hydroforming of basketball and orange spherical shells. According to the obtained results, the basketball shell under the same internal pressure had a more accurate shape and more uniform thickness than the orange shell. They concluded that hydroforming the basketball preform is well established and is an appropriate preform for producing a spherical shell. Zhang et al. [18] evaluated the buckling properties of externally pressurized bulged barrels and the bulging performance of internally pressurized cylindrical preforms. The cylindrical preforms had a thickness-to-radius ratio of 0.0176 and height-to-radius ratio of 1.961. The bulging and buckling were numerically evaluated for several bulging magnitudes. The results indicate that this forming technique can be extended to fabricate typical externally pressurized vessels such as barreled pressure hulls. In addition, the external pressure-supporting capacity of the bulged vessels was substantially enhanced by increasing the material hardening and curvature. Yang et al. [19] proposed an IHBF method using a triangular patch polyhedron as the closed preform shell. When triangular flat parts are welded along the edges in sequence, triangular patch polyhedrons are formed naturally. From the radius of the spherical pressure vessel, a design formula was derived to calculate the side lengths of the triangular flat-plate parts. The water pressure, volume, average strain of molding, and amount of spring-back after molding, which are necessary for implementing the IHBF for practical use, were also formulated. The process directly utilizes triangular flat plate parts, eliminating the need for molds to process closed preform shells and resulting in a low average plastic strain during forming, thereby improving the quality of the formed spherical pressure vessels. Zhang et al. [20] studied the free hydroforming of stainless-steel egg-shaped shells theoretically and experimentally. The equivalent stress, yielding load, and inscribed segmented preform of the egg-shaped shells were investigated. The nonlinear finite element method was used to analyze the hydroforming of egg-shaped shells. They showed that free hydroforming can be an effective technique for manufacturing egg-shaped pressure hulls and can produce shells with high revolution symmetry, irrespective of the geometric deviation of the segmented preform.

In this study, the IHBF of a spherical vessel was studied through experimental and numerical approaches. The geometric accuracy of the formed vessel, thickness distribution along the equatorial and meridian paths, and critical fluid pressure at which instability occurs were evaluated. The effects of the number of lateral petals on the thickness distribution of the formed vessel, the geometric accuracy, and the critical fluid pressure were investigated.

## 2. Experimental Procedure

A spherical vessel with a diameter of 400 mm consisting of 12 lateral petals and two circular plates with a diameter of 50 mm at the poles of the vessel was formed in the experimental study. A schematic of the vessel is shown in Fig. 1. A low-carbon steel St12 sheet

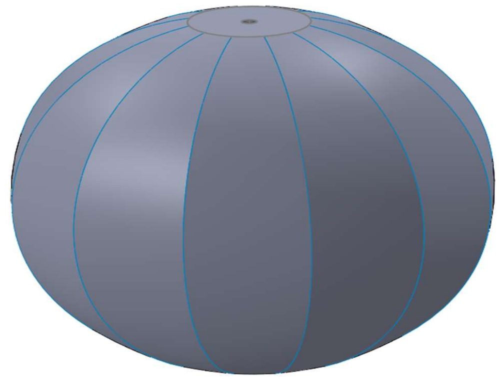

**Fig. 1.** Geometry of final workpiece.

with a thickness of 0.8 mm was used. Uniaxial tension tests were performed according to ASTM-A370 to determine the material properties of the sheet (Table 1).

**Table 1.** Mechanical properties of sheet

| Materials | Carbon Steel St12 |
|---|---|
| Modulus of elasticity (MPa) | 210000 |
| Poisson’s ratio | 0.3 |
| Yield stress (MPa) | 190 |
| Strength coefficient (MPa) | 510 |
| Strain hardening, *n* | 0.2 |

To manufacture the spherical vessel, 14 segments were first cut according to the designed patterns and preformed. A CNC laser cutting machine was used to cut the segments. Preformed lateral petals and two circular plates were fabricated and welded using the tungsten inert gas (TIG) welding method. A 1 mm diameter ER70S filler rod was used in the TIG welding process. In this study, to measure the thickness distribution of the micrometer with an accuracy of 0.001 mm and the cross-sectional profile of the spherical shell, a measuring watch with an accuracy of 0.01 mm was used. Finally, the spherical vessel was formed by applying hydraulic pressure using a hydraulic pressure unit with a maximum applicable fluid pressure of 25 MPa. The maximum hydraulic pressure applied to the vessel was controlled using a pressure-control valve. SAE20W50 oil was used as hydraulic fluid. A vessel was successfully formed at a pressure of 1.1 MPa. Fig. 2 shows the manufacturing process of the workpiece in the form of a flowchart. Fig. 3 shows the experimental equipment and forming process of the experimental specimens.

Fig. 4 shows the formed spherical vessel cut for geometrical and dimensional measurement and evaluation of the thickness distribution in the equatorial and meridian directions.

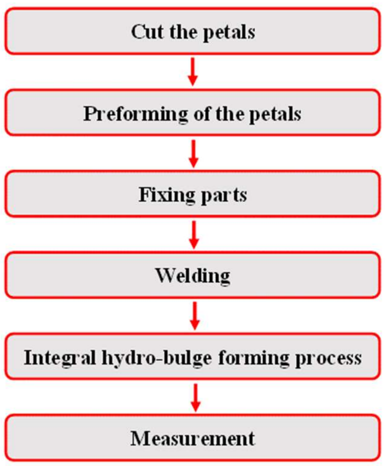


**Fig. 2.** Manufacturing process of the workpiece.

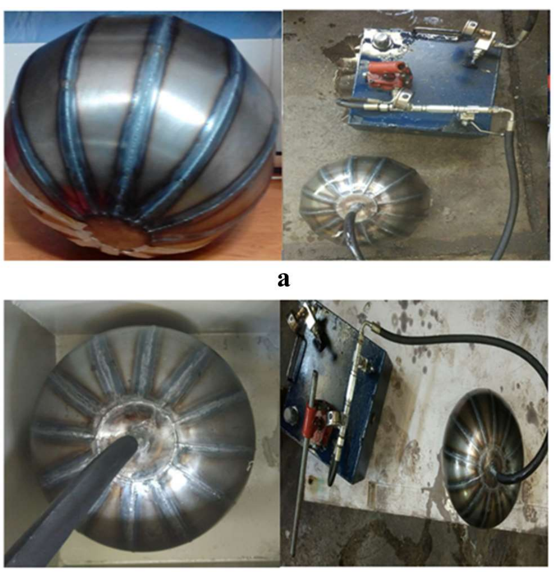


**Fig. 3.** Hydro-bulging of a spherical shell with 12 lateral petals: (a) before, and (b) after the hydro-bulging process.

**Fig. 4.** The formed vessel cut for measurements.

## 3. Finite Element Simulation

A numerical study of the IHBF of a spherical vessel was performed using the ABAQUS/Explicit code. The dimensions of the final workpiece were as described in section 2. In the numerical study, spherical vessels were simulated using different numbers of lateral petals. Therefore, depending on the number of petals, one-half or one-eighth of the vessels were modeled. The mechanical properties of the metallic sheets are presented in Table 1. The sheets were modeled as deformable parts with 4-node shell elements (S4R). The liquid was not modeled; instead, an internal pressure with a uniform distribution was applied. The internal pressure was linearly increased to the determined limit in order to achieve the desired dimensions and geometry. Quasi-static conditions were also considered. To reduce the computational time, the analysis time was considered to be a fraction of the actual process, and care was always taken to ensure that the amount of kinetic energy of the deformation did not exceed five percent of the internal deformation energy. Fig. 5 shows the meshing style of the specimen and deformed specimen with 12 lateral petals.

Bifurcation theory was used to determine the forming limit of the numerical simulation. In bifurcation theory [21], to observe the onset of localized necking, we can refer to the diagrams of the second differentiation of thickness with respect to time and abrupt change in thickness strain. According to the structural symmetry in the spherical shell in the cut boundaries, the boundary condition of symmetry has been applied, and depending on which coordinate axis the normal of the plane of

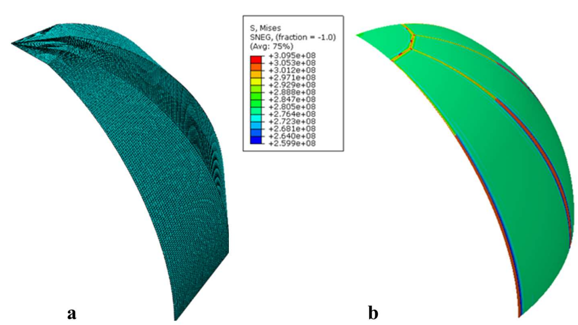


**Fig. 5.** The (a) meshing style of the specimen, and (b) deformed specimen with 12 lateral petals.

symmetry is selected, from the constraints of XSYMM, YSYMM, and ZSYMM are used in a spherical shell, which is modeled as one-eighth of all three; the above constraint and in the spherical shell, which is modeled as a half, are only from the YSYMM symmetry constraint used. Loading involves the application of pressure to the inner surface of the spherical shell. The amount of pressure versus time in the analysis increased linearly, and to adjust this mode, the pressure value in the range section to a table in which the amount of fluid pressure during the forming step was specified with a coefficient of the maximum fluid pressure entered into the software. To obtain the optimal dimensions and number of elements, models with different granularity numbers were simulated, and the results were analyzed. Mesh sensitivity analysis was performed to determine the optimal granulation size. Moreover, the effect of the amount of granularity was compared on the process analysis time in different modes, and finally, after examining the results, a value of 0.195 mm was considered for the mode of one-eighth sphere, and 15000 elements were created on the model. In addition, a value of 1.7 mm was considered for the case of one-half of the sphere, and 60000 elements were created on the model.

## 4. Results and Discussion

Fig. 6 depicts the cross-sectional profile of the formed vessel with 12 lateral petals obtained from the numerical simulation compared with those measured in the real experiment. The cross-section predicted numerically simulated cross-section is in good agreement with the experimental results. The maximum deviation between the numerical and experimental profiles is 6%.

Fig. 7 shows a comparison of the thickness distributions along the equatorial line for a quarter of the formed vessels with 12 lateral petals obtained numerically and experimentally. A logical agreement was observed among the numerical and experimental results. Maximum thinning occurred at the center of the petals.

Fig. 8 compares the experimental and numerical results for the thickness distribution along the meridian path from the pole to the equator for a spherical vessel with 12 lateral petals. The maximum and minimum thickness reductions occurred at the equatorial region and pole of the vessel, respectively.

The effects of the number of lateral petals on the sphericity of the hydro-bulged vessel were investigated numerically for vessels made of 0.8 mm, 1 mm, and

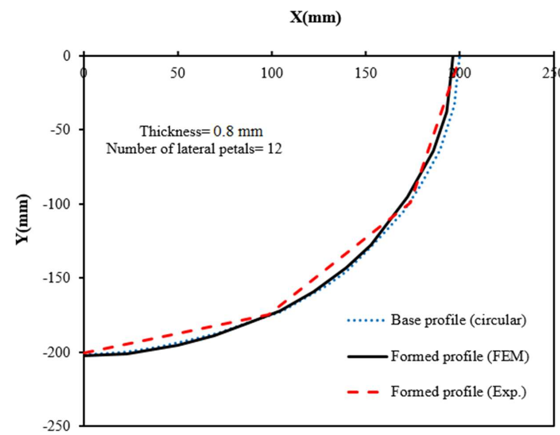


**Fig. 6.** Comparison of cross-sectional profiles in the equatorial between experimental and numerical analysis results.

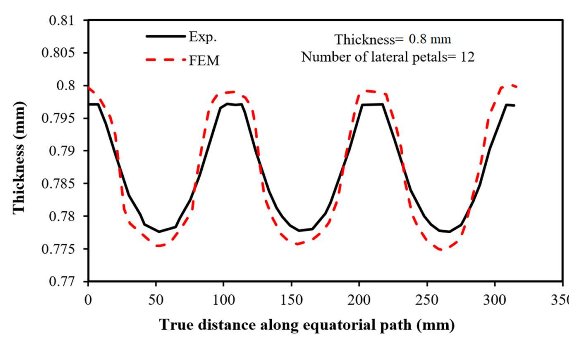


**Fig. 7.** Comparison between numerical and experimental results of thickness distribution per 3 lateral petals along the equatorial path of the spherical shell.

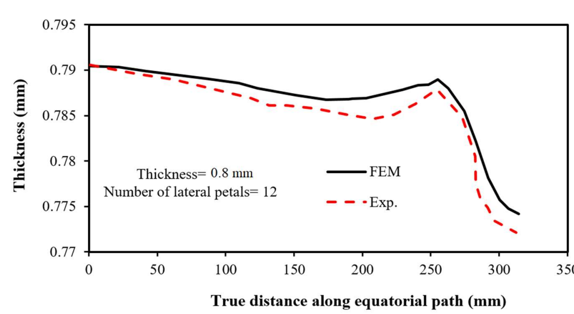


**Fig. 8.** Comparison between numerical and experimental results of thickness distribution along the spherical shell meridian path.

1.2 mm thick sheets. Fig. 9 illustrates the effect of the number of lateral petals on the deviation from the spherical form of the vessel. As can be seen, increasing the number of lateral petals reduced the deviation from the spherical form. In other words, the use of more lateral petals in the preform provides a higher geometric accuracy in the form of a vessel.

The effect of the number of lateral petals on the thickness distribution in the equatorial direction is shown in Figs. 10 and 11. Figs. 10(a) and 10(b) show the thickness distributions in the equatorial line for a quarter of the formed vessels with 8, 10, and 12 lateral petals made of 0.8 mm and 1 mm thick sheets. The results indicate that the maximum reduction in thickness occurs when 8 lateral petals are used, and the minimum thickness reduction is related to the case where 12 lateral petals are used. However, it appears that the uniformity of the thickness distribution of the vessel is directly related to the number of lateral petals. The use of more lateral petals leads to a more uniform thickness distribution of the hydro-bulged vessel.

Fig. 10 shows the same results as Fig. 9 for one-half of the vessels with 9, 13, and 17 lateral petals of 1 mm thickness. The increase in the number of lateral petals will reduce the thickness variation of the formed vessel and results in a more uniform thickness distribution.

The influence of the number of lateral petals on the critical fluid pressure is shown in Fig. 12. Localized necking occurs at this critical pressure; therefore, to form a rupture-free vessel, the internal pressure during the bulging process should not exceed this critical value. As expected, if the sheet thickness increases, the critical

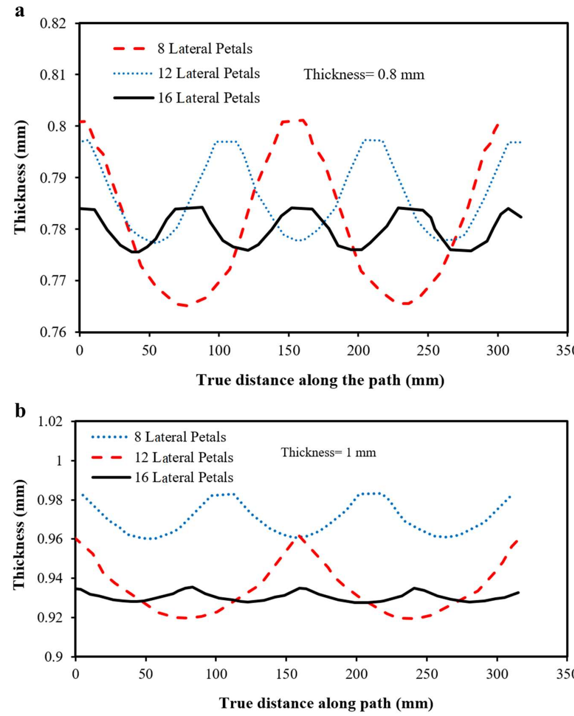


**Fig. 10.** (a) Equilibrium thickness distribution for 8, 12, and 16 side petals at a fixed thickness of 0.8 mm. (b) Equilibrium thickness distribution for 8, 12 and 16 side petals at a constant thickness of 1 mm.

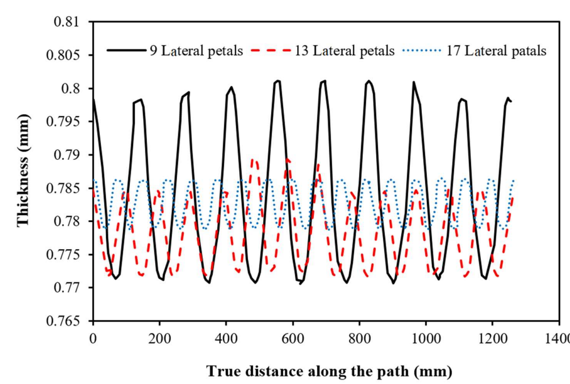


**Fig. 11.** Thickness distribution in the equatorial for the number of odd petals.

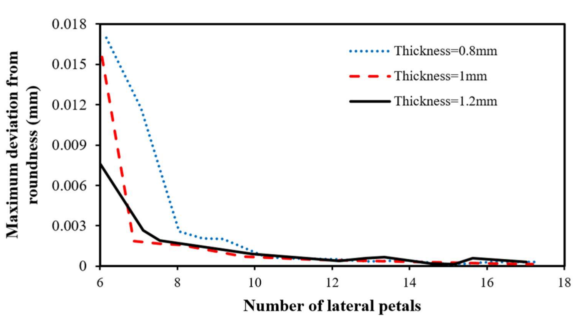


**Fig. 9.** The effect of the number of lateral petals on the maximum diversion from the round shape.

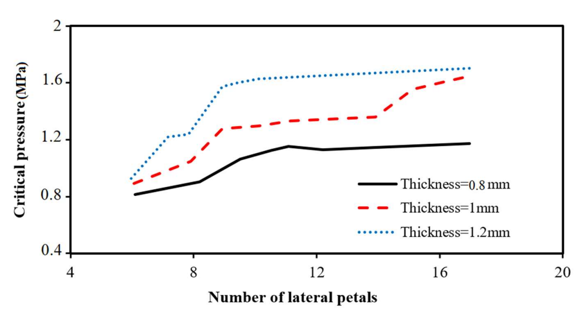


**Fig. 12.** The effect of the number of lateral petals on the critical pressure.

fluid pressure will increase as well. As shown in Fig. 11, increasing the number of lateral petals leads to the increase in the critical fluid pressure at which instability occurs.

## 5. Conclusion

The integral hydro-bulge forming of spherical vessels was numerically and experimentally studied. A numerical simulation was performed using the Abaqus/Explicit code. An experiment is also conducted. The validity of the numerical results was examined by comparing them with the experimental results. The influence of the number of lateral petals on the thickness distribution along the equatorial and meridian paths, the sphericity of the formed vessel, and the critical fluid pressure at which instability occurs were investigated. The following conclusions can be drawn from this study:

1. Along the equatorial line of the spherical vessel, maximum thickness reduction occurred at the center of the petals. The maximum thickness reduction will occur in the 8-petal state and the least thickness reduction will occur in the 12-petal state.
2. Along the meridian path, the maximum and minimum thinning occurred at the equatorial region and pole of the formed vessel, respectively. By increasing the number of petals from 8 to 16, the thickness decreases by 4.2%.
3. The deviation of the hydro-bulged vessel from the spherical form was reduced by using more lateral petals. For example, the maximum diversion from a round shape for a spherical shell had eight lateral petals equal to 2.6 mm, which, by doubling the number of lateral petals, will reach 0.2. The largest diversion of the shape decreased by 92%.
4. The number of lateral petals directly affects the uniformity of thickness distribution. The use of more lateral petals resulted in a more uniform thickness distribution of the formed vessel.
5. The critical fluid pressure at which instability occurs was increased by increasing the number of lateral petals. By doubling the number of lateral petals, the fracture pressure will increase by 74%.

## Conflict of Interests

The authors have no relevant financial or non-financial interests to disclose.

## Funding

The authors declare that no funds, grants, or other support were received during the preparation of this manuscript.

## 6. References

[1] H. Deilami Azodi, S. Rezaei, A. Zeinolabedin Beygi, H. Badparva, Investigation of parameters influencing forming force and thickness distribution in single point incremental forming of AA3105-St12 two-layer sheet, *Iranian Journal of Materials Forming,* 9(2) (2022) 46-57.

[2] H. Talebi-Ghadikolaee, H. Moslemi Naeini, A.H. Rabiee, A. Zeinolabedin Beygi, S. Alexandrov, Experimental-numerical analysis of ductile damage modeling of aluminum alloy using a hybrid approach: ductile fracture criteria and adaptive neural-fuzzy system (ANFIS), *International Journal of Modelling and Simulation*, (2022) 1-16.

[3] H. Deilami Azodi, A. Hassani, S. Mazdak, A. Zeinolabedin Beygi, E. Sherkatghanad. Numerical study on weld line displacement in rubber pad forming of tailor welded blanks, *Karafan Quarterly Scientific Journal*, 19(1) (2022) 145-164.

[4] M.S. Zeinali, H.M. Naeini, H. Talebi-Ghadikolaee, V. Panahizadeh, Numerical and experimental investigation of fracture in roll forming process using Lou–Huh fracture criterion, *Arabian Journal for Science and Engineering*, 47(12) (2022) 15591-15602.

[5] M. Molaei, M. Safari, H. Deilami Azodi, J. Shahbazi Karami, Experimental and numerical investigations of hydromechanical deep drawing of a bilayer conical cup, *Journal of Stress Analysis*, 3(1) (2018) 53-60.

[6] M. Safari, S.M. Miralaa, R. Alves de Sousa, Experimental investigation of the effects of process parameters on the radius of curvature in laser forming process of cylindrical surfaces, *Metals*, 13(1) (2023) 56.

[7] C. Bell, J. Corney, N. Zuelli, D. Savings, A state of the art review of hydroforming technology: Its applications, research areas, history, and future in manufacturing, *International Journal of Material Forming*, 13 (2022) 789-828.

[8] S. Zhang, Z.R. Wang, T. Wang, The integrally hydroforming process of spherical vessels, *International Journal of Pressure Vessels and Piping*, 42(1) (1990) 111-120.
[9] S. Zhang, Z.R. Wang, Further investigation into the hydro-bulging process for 32-sided polyhedral shells, *Journal of Materials Processing Technology*, 31(1-2) (1992) 169-177.
[10] B.G. Teng, S.J. Yuan, Z.R. Wang, Experiment and numerical simulation of hydro-forming toroidal shells with different initial structure, *International Journal of Pressure Vessels and Piping*, 78(1) (2001) 31-34.
[11] W. Hu, Z.R. Wang, Deformation analyses of the integrated hydro-bulge forming of a spheroidal vessel from different preform types, *Journal of Materials Processing Technology*, 151(1-3) (2004) 275-283.
[12] Z.R. Wang, G. Liu, S.J. Yuan, B.G. Teng, Z.B. He, Progress in shell hydroforming, *Journal of Materials Processing Technology*, 167(2-3) (2005) 230-236.
[13] S.J. Yuan, L. Hu, Z.B. He, B.G. Teng, Z.R. Wang, Research on two-step hydro-bulge forming of ellipsoidal shells with large axis length ratio, *Journal of Harbin Institute of Technology*, 20(3) (2013) 93-98.
[14] S.J. Yuan, W.W. Zhang, B.G. Teng, Research on hydro-forming of combined ellipsoidal shells with two axis length ratios, *Journal of Materials Processing Technology*, 219 (2015) 124-132.
[15] Q. Zhang, Z.R. Wang, Shape improvement of a dieless hydro-bulged sphere made of hexagonal and pentagonal shaped panels, *Journal of Materials Processing Technology*, 220 (2015) 87-95.
[16] W.W. Zhang, S.J. Yuan, Pre-form design for hydro-forming process of combined ellipsoidal shells by response surface methodology, *The International Journal of Advanced Manufacturing Technology*, 81 (2015) 1977-1986.
[17] R. Zhang, W.W. Zhang, S.J. Yuan, Research on hydro-forming of spherical shells with different preform types, *The International Journal of Advanced Manufacturing Technology*, 92 (2017) 2631-2638.
[18] J. Zhang, F. Wang, F. Wang, X. Zhao, W. Tang, F. Chen, Buckling properties of bulged barrels under external pressure, *Thin-Walled Structures*, 168 (2021) 108226.
[19] Y. Jing, C. Kong, J. Guan, W. Zhao, X. Zhao, Integral hydro-bulge forming method of spherical pressure vessels using a triangle patch polyhedron, *Journal of Pressure Vessel Technology*, 145(3) (2023) 031303.
[20] J. Zhang, M. Dai, F. Wang, W. Tang, X. Zhao, Y. Zhu, Theoretical and experimental study of the free hydroforming of egg-shaped shell, *Ships and Offshore Structures*, 17(2) (2022) 257-267.
[21] S. Stören, J.R. Rice, Localized necking in thin sheets, *Journal of the Mechanics and Physics of Solids*, 23(6) (1975) 421-441.